Chapter 2
A Numerical Study on the Potential of Acoustic Metamaterials

Fabian Duvigneau and Sascha Duczek

Abstract In the present contribution we are going to investigate a special class of acoustic metamaterials, i.e. synthetic foams with spherical inclusions. This study is motivated by the need for an improved acoustical behavior of engines and vehicles which is one important criterion for the automotive industry. In this context, innovative materials offering a high damping efficiency over a wide frequency range are becoming more and more important. Since there is an innumerable selection of different absorbing materials with an equally large range of properties numerical studies are inevitable for their assessment. In the paper at hand, we look at a special class of such materials in which the influence of the inclusions on the acoustical behavior is examined in detail. To this end, we vary the size, mass density, number and position of spherical inclusions. Here, the main goal is to improve the damping properties in comparison to conventional materials which can be bought off the shelf. In that regard, the lower frequency range is of special interest to us. The results show that a random distribution of the inclusions should be favored while for the other parameters values that are centered within the investigated interval are recommended.

2.1 Introduction

In general, there are two main approaches for improving the acoustic behavior of arbitrary parts: (*i*) active and (*ii*) passive methods. Active methods require an external energy supply in order to drive actuators that are able to excite the structure and create destructive interferences of elastic and acoustic waves (Gabbert et al, 2017). To achieve an efficient damping the vibrations of the structure have to be measured first before a suitable control strategy can be applied. A wide variety of control concepts

Fabian Duvigneau · Sascha Duczek
Institut für Mechanik, Otto-von-Guericke-Universität Magdeburg, Universitätsplatz 2, 39106 Magdeburg, Germany
e-mail: fabian.duvigneau@ovgu.de, sascha.duczek@ovgu.de

H. Altenbach et al. (eds.), *Analysis and Modelling of Advanced Structures and Smart Systems*, Advanced Structured Materials 81,
https://doi.org/10.1007/978-981-10-6895-9_2

with automotive applications can be found in the literature, e.g., active structural acoustic control (ASAC) of an oil pan (Ringwelski et al, 2011), active noise control (ANC) of the cabin noise within a car (Schirmacher et al, 2007) or active vibration control (AVC) of a rear axle to avoid gear whining (Troge et al, 2016). However, today passive concepts are still more popular in industrial applications due to their inherent simplicity, the absence of an additional energy supply, the costs, the failure safety and the fact that active concepts are only efficient in the low frequency range.

In the context of passive methods the geometry of the part is often modified to eliminate sound transmission paths and hence, to reduce the resulting sound radiation of the structure. This can be achieved by adding mass or stiffeners to specific locations where also alternative materials, such as synthetic or metal foams (Schrader et al, 2015), are employed. In the wide body of literature also more exotic approaches such as the use of granular materials (Duvigneau et al, 2016a) can be found. Here, a sandwich panel with a honeycomb core was utilized to intelligently distribute the granular material. This methodology leads to an improved damping behavior in conjunction with a high stiffness to mass ratio (Koch et al, 2017b). In this context, it was shown that a granular medium made of light and highly elastic rubber is very effective for vibration damping (Koch et al, 2017a).

Even today it is unfortunately still common practice to focus on targets such as fuel consumption, power output, mass and design aspects when optimizing automotive parts. In this context the acoustic performance of vehicles is often neglected and therefore, we need concepts to tackle this issue after the final design has already been approved. Typically acoustic problems are only detected experimentally when an expensive prototype has been build and an extensive testing campaign is conducted. At this stage in the development process it is, however, almost prohibitive to propose fundamental changes in the design and hence, alternative methods need to be employed until the acoustic behavior is finally part of initial considerations. First steps in this direction are taken in Duvigneau et al (2016b,d), where a holistic workflow for the acoustic evaluation of a combustion engine is developed. However, nowadays it is still common practice to mitigate observed acoustic problems of prototypes by applying damping materials to acoustically conspicuous components. In Duvigneau et al (2016c) it is exemplarily shown that an encapsulation of an engine is a very efficient approach to significantly reduce the noise emission of a vehicle. Here, the main challenge is to balance the need for an improved acoustic emission behavior with mass considerations. The additional mass caused by the installation of an encapsulation should be naturally as low as possible. An additional consideration is the available space which is in modern vehicles rather limited such that the dimensioning of the encapsulation needs to be adapted to these requirements.

Due to the mentioned issues one important aspect when designing passive noise reduction approaches is to improve the damping properties of the deployed materials. They need to have a high damping ratio over a wide frequency range while being both light and thin. The classical approach for noise control applications is to utilize homogeneous heavy foils made of high density viscoelastic materials such as bitumen or butyl rubber. These foils are mainly applied at locations where the noise emission is rather high such as large planar faces. Here, they increase the transmission loss through material damping (described by the loss factor) and the additional mass (lower vibration amplitudes). Because of the large-area application of these materials there is still quite some room for improvement left. Therefore, heterogeneous materials have been in the focus of investigations recently. Such material systems include polyurethane (PUR) and melamine foams or microfiber materials which provide a high material damping due to the additional interactions at the fluid-solid-interface. Their advantage compared to previously discussed materials is the comparably low density (which naturally leads to low mass gains). Generally speaking, the characteristic value of the acoustic effect, provided by homogeneous materials, is governed by the thickness only, whereas porous (heterogeneous) materials offer much more freedom to be tailored for specific applications. Parameters such as the mean pore size, the porosity (volume fraction) and the reticulation rate can significantly influence the acoustic performance. These influence parameters can be adjusted by chemists or process engineers during the manufacturing process. By adding an additional mass layer at the surface of the heterogeneous material the dissipation effect is increased even further. Now, the material system represents a mass-spring-damper system. These bimaterial foam systems have been extensively investigated in a previous study (Schrader et al, 2016). A remarkable feature of the investigated foams is that the added mass layer is created by impregnating only a part of the base material. This procedure is very flexible in terms of penetration depth and achievable density.

Special classes of heterogeneous materials are the so-called acoustic metamaterials. In the following, we discuss an important group of these metamaterials, which is made of locally resonant structures. Generally, they consist of a soft matrix phase featuring stiff mass inclusions with different weights and sizes. In various studies it has been shown that the mass inclusions within the elastic matrix cause frequency bands with high transmission losses or absorption coefficients (Liu et al, 2000, 2005; Fuller and Saux, 2012; Idrisi et al, 2010; Deymier, 2013; Sheng et al, 2017; Lu et al, 2009); this behavior is analogous to bandgap phenomena in phononic crystals (Jensen, 2011; Zhang et al, 2006; Zhao et al, 2013). The frequency bands with increased transmission losses depend on both the mass of the inclusion and its location (Fuller and Saux, 2012; Idrisi et al, 2010; Deymier, 2013). One important feature that is demonstrated in the cited literature is the ability to increase the transmission loss especially in the low frequency range where classical passive approaches do not work satisfactorily. Therefore, a simple inclusion of "resonant" masses within a conventional damping material can lead to significant gains in terms of the suppression of sound emission. In general, it is suggested to distribute inclusions with different masses at various locations within the elastic matrix to achieve a notable sound energy dissipation in a broader frequency range.

Another approach to design metamaterials has been introduced in Sui et al (2015). Here, a lightweight honeycomb structure was covered with an elastic membrane. This material shows a high transmission loss at low frequencies which can be attributed to the effect of the membrane. In Schrader et al (2017a) this method was seized and combined with two additional metamaterial concepts. First, only the honeycomb-membrane system was investigated to obtain reference measurements. In a second step the honeycombs were filled with PUR foam. Finally, mass inclusions were placed in the honeycomb cells before filling these cells with foam as in the previous step. Honeycomb structures combined with PUR foam show significant sound pressure level reductions in a frequency range from 0.5 to 2 kHz. These reductions are notably higher than the ones gained with a simple PUR foam of the same thickness. The honeycomb plate with the surface membrane alone does not show these effects either. A further improvement is gained by the use of the mass inclusions within the honeycombs, especially the concept with a large number of small-sized mass inclusions surrounded by the PUR foam shows a high sound pressure level reduction.

In Schrader et al (2017a) also another concept which is inspired by applications in room acoustics has been proposed. The fundamental idea is based on the application of perforated acoustic panels which contain large air cavities beyond the interface. In this concept the energy is dissipated by friction between the moving air particles and the solid perforated plate. Schrader et al (2017a) applied this idea to PUR foams. In their approach large cavities were introduced into the foam structure and covered by micro-perforated membranes. The membrane was micro-perforated, as the perforations have to be rather small in order to devise an efficient material system (Fuchs, 2007). The operating principle is based on the physical concept of a Helmholtz resonator whose efficiency depends on the friction losses in the micro-perforations. The theory of noise reduction by micro-perforated absorbers was originally developed by Maa (1998). This idea was further extended by Zhang and Gu (1997) who suggested employing a structure featuring a double-layered micro-perforated absorber. The specific feature of such a design is that it exhibits two absorption maxima.

In the present contribution a metamaterial based on spherical inclusions that combines the benefits of a low mass density with an improved noise absorption compared to conventional damping materials (especially at low frequencies) is proposed and studied in detail. In Fig. 2.1 a possible design of the proposed metamaterial which is attached to a rectangular plate is shown. Here, three layers of inclusions which are distributed in a structured fashion are depicted. The investigated material system increases the energy dissipation within the polyurethane base material (foam) by adding additional masses. The basic idea is to create a local mass-spring-damper system which is able to attenuate the vibrations. In the following sections the acoustic efficacy of the proposed metamaterial is investigated for several configurations differing in weight, size and location of the spherical inclusions within the PUR foam.

2.2 Models for the Parametric Studies

In this section the road map for our numerical investigations is explained, the used models are presented and in the following Sect. 2.3 selected results that are representative of the behavior for the proposed metamaterial are discussed. The results are obtained by numerical simulations using the finite element method (FEM)

(Zienkiewicz and Taylor, 2000; Hughes, 1987) which is the dominating tool to solve partial differential equations arising in many different branches of engineering.

In Fig. 2.2 the setup for the numerical experiments is depicted. On the left hand side the FE-model of the plate with the metamaterial attached to its surface is shown. The dimensions of the model are compiled in Table 2.1. In this model structural

Table 2.1: Dimensions of the structural model

	length	width	thickness t
Aluminum plate	440 mm	240 mm	5 mm
Metamaterial	400 mm	200 mm	40 mm

damping is used, which assumes that the damping forces F_D are opposed to the velocity and are proportional to the forces F_S caused by stressing the structure. The damping forces are $F_D = i \cdot \delta \cdot F_S$ wherein δ is the structural damping factor and i is the imaginary unit. The corresponding damping factors δ of the different materials, which are used within the FE-model, are listed in Table 2.2. As Dirichlet boundary conditions we fixed the displacements in all spatial directions at the four corner nodes

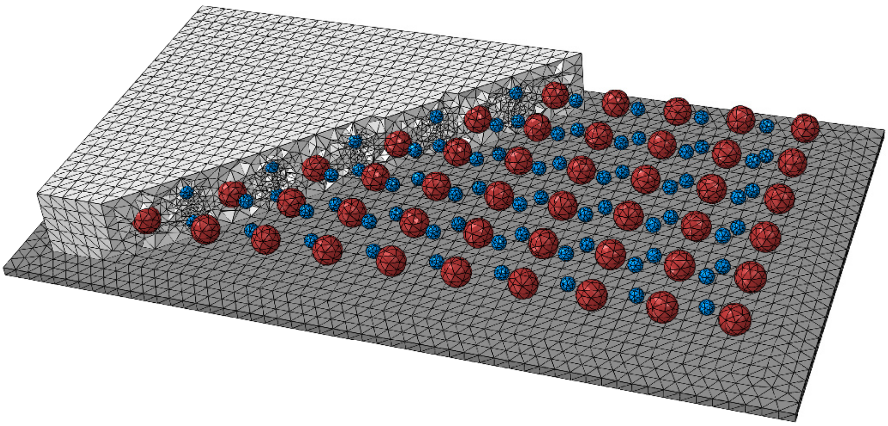

Fig. 2.1: Example of an acoustic metamaterial attached on a rectangular plate

Table 2.2: Material properties of the numerical reference model

	aluminium	foam	inclusions
Young's modulus	70000 N/mm^2	5 N/mm^2	5000 N/mm^2
Density	2.7 g/cm^3	0.05 g/cm^3	0.5 g/cm^3
Poisson ratio	0.3	0.3	0.3
Structural damping	0.01	0.05	0.0

of the backside of the aluminum plate. In experiments the excitation is typically applied by means of a shaker and therefore, we introduce the Neumann boundary conditions by attaching an aluminum cylinder (height: 10 mm, radius 5 mm) at the centroid of the backside of the aluminum plate. This procedure is identical to the experimental setup that was used in a previous study (Schrader et al, 2017b). A white noise signal with an amplitude of 1 N is generated to excite the structure in the whole frequency range of interest. The numerical analysis is executed in the frequency domain due to the computational costs of a fully transient analysis in the time domain.

On the right hand side of Fig. 2.3 the FE-model of the air volume surrounding the structure is depicted. The spherical air volume needed to compute the sound pressure distribution has a radius of 330 mm. Consequently, for frequencies higher than 1.55 kHz the far field assumption (approximately 1.5 times the wavelength) already holds within the discretized domain. To reduce the computational effort the surrounding fluid volume is modeled only as a hemisphere. Due to the geometric complexity of the micro-structure of metamaterials both the structural and the acoustic domain are discretized by means of tetrahedral finite elements with quadratic shape functions (10-node tetrahedra). The maximum element size of the structural model is set to 8 mm which corresponds to 8 nodes per wavelength of the maximum

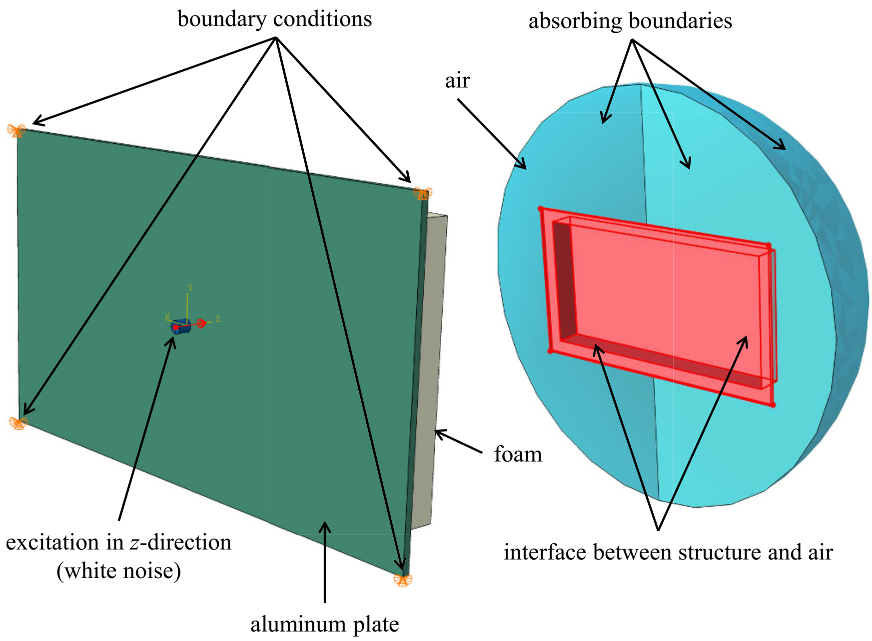

Fig. 2.2: Simulation model of the plate, foam and air including interface and boundary conditions

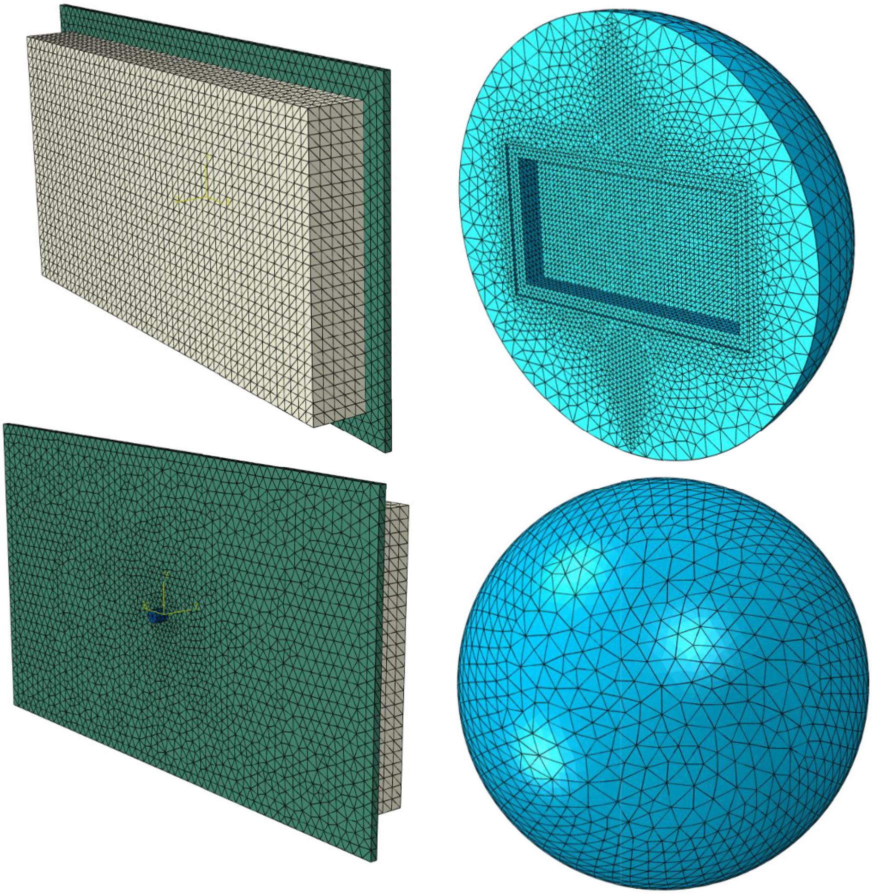

Fig. 2.3: FE-models of the aluminum plate with the attached foam layer and the surrounding air

frequency. At the interface between both models (structural-acoustic interface) a conforming mesh is generated and the element size is then slowly increased towards the periphery of the hemisphere where a maximum element size of 30 mm is reached. In Duvigneau (2017) it was shown that this discretization is still reasonable due to the much finer discretized interface. For the acoustic problem free-field conditions are assumed and therefore, the outer boundary of the air volume are modeled as absorbing boundaries (impedance based absorbing boundary conditions(Givoli, 2008)). At the structural-acoustic interface the air is excited through the surface velocities of the vibrating structure, which have been calculated in a previous analysis step. Due to the conformal interface mesh the interpolation of the results is trivial. To further reduce the computational effort an uncoupled acoustic simulation is executed, i.e. the influence of the vibrating air on the aluminum plate and the metamaterial is neglected. The geometrical dimensions, the mesh parameters, the boundary and loading conditions are identical for all investigated configurations. Thus, we ensure that the results are comparable as the only influence is now related to the changes made with respect to the metamaterial. Here, we primarily change the geometry (volume), distribution (number, location) and material properties (density, Young's modulus) of the spherical inclusions.

In Table 2.2 the material properties of aluminum, PUR foam and the initial data for the inclusions are compiled. If not stated otherwise this data set is used in all numerical simulations. For the sake of clarity, all important parameters describing the models used in our numerical analyses in Sect. 2.3 are compiled in Table 2.3. Here, all details such as the number of spherical inclusions, their diameter and their material properties (mass density ϱ, Young's modulus E) are listed. Note, that the Poisson's ration ν is set to 0.3 for all constituents (see Table 2.2). From these information the additional mass can be computed, although we have to bear in mind that the mass of the fully foam filled structure needs to be taken into consideration. That means that we have to compute the mass of the inclusions and subtract the mass of the foam that originally occupied this space. The values Δx, Δy and Δz describe the spacing between adjacent spheres measured from centroid to centroid (for structured arrangements only). If only one layer of spheres is deployed Δz gives the distance between the centroid of the sphere and the bottom surface of the foam structure.

2.3 Numerical Results

In the current section we comprehensively discuss selected results of our numerical investigations that are representative of the behavior of the proposed metamaterial.

2.3.1 Influence of the Distribution of the Spherical Inclusions

In this section we investigate six different configurations which are depicted in Fig. 2.4. All models contain 50 spherical inclusions with a diameter of 15 mm while only their distribution (with respect to the location) is varied. One important question we want to answer by executing this study is whether the positioning with respect to the out-of-plane direction (z-axis, height) or the in-plane positioning (x-y-plane) is more significant for the damping behavior. In a previous investigation (Schrader et al, 2017b) it was suggested that the former effect would be dominant.

Table 2.3: Parameters for the numerical models used in the parametric investigations. The spacing of the inclusions is given in terms of the variables $a = 36.4$ mm, $b = 33.3$ mm and $t = 40$ mm (thickness of the metamaterial).

#	Geometry	Number of inclusions	Diameter	Mass density	Young's modulus	Added mass	Δx	Δy	Δz
Sect. 2.3.1									
1	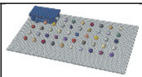	50, 1 layer 5x10	15 mm	0.5 g/cm^3	5,000 N/mm^2	39.8 g	a	b	$0.5t$
2	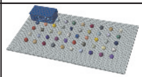	50, 1 layer 5x10	15 mm	0.5 g/cm^3	5,000 N/mm^2	39.8 g	a	b	$0.25t$
3	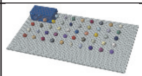	50, 1 layer 5x10	15 mm	0.5 g/cm^3	5,000 N/mm^2	39.8 g	a	b	$0.75t$
4	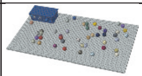	50, random distribution in-plane	15 mm	0.5 g/cm^3	5,000 N/mm^2	39.8 g	-	-	$0.5t$
5	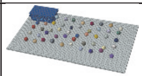	50, random distribution out-of-plane	15 mm	0.5 g/cm^3	5,000 N/mm^2	39.8 g	a	b	-
6	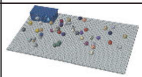	50, random distribution in all directions	15 mm	0.5 g/cm^3	5,000 N/mm^2	39.8 g	-	-	-
Sect. 2.3.2									
7	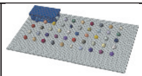	50, 1 layer 5x10	15 mm	0.1 g/cm^3	5,000 N/mm^2	4.42 g	a	b	$0.5t$

Continued on next page...

Table 2.3 – continued from previous page.

#	Geometry	Number of inclusions	Diameter	Mass density	Young's modulus	Added mass	Δx	Δy	Δz
8	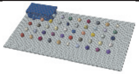	50, 1 layer 5x10	15 mm	1.0 g/cm^3	5,000 N/mm^2	83.9 g	a	b	0.5t
9	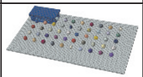	50, 1 layer 5x10	15 mm	5.0 g/cm^3	5,000 N/mm^2	437.4 g	a	b	0.5t
10	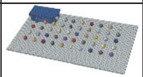	50, 1 layer 5x10	15 mm	0.5 g/cm^3	500 N/mm^2	39.8 g	a	b	0.5t
11	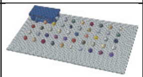	50, 1 layer 5x10	15 mm	0.5 g/cm^3	50,000 N/mm^2	39.8 g	a	b	0.5t
Sect. 2.3.3									
12	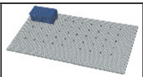	50, 1 layer 5x10	5 mm	13.5 g/cm^3	5,000 N/mm^2	39.8 g	a	b	0.5t
13	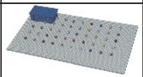	50, 1 layer 5x10	10 mm	1.6875 g/cm^3	5,000 N/mm^2	39.8 g	a	b	0.5h
14	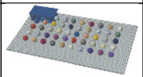	50, 1 layer 5x10	20 mm	0.2109 g/cm^3	5,000 N/mm^2	39.8 g	a	b	0.5t
15	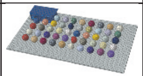	50, 1 layer 5x10	25 mm	0.108 g/cm^3	5,000 N/mm^2	39.8 g	a	b	0.5t

Continued on next page...

Table 2.3 – continued from previous page.

#	Geometry	Number of inclusions	Diameter	Mass density	Young's modulus	Added mass	Δx	Δy	Δz
Sect. 2.3.4									
16	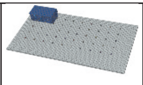	50, 1 layer 5x10	5 mm	0.5 g/cm^3	5,000 N/mm^2	1.47 g	a	b	0.5t
17	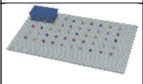	50, 1 layer 5x10	10 mm	0.5 g/cm^3	5,000 N/mm^2	11.8 g	a	b	0.5t
18	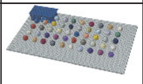	50, 1 layer 5x10	20 mm	0.5 g/cm^3	5,000 N/mm^2	94.2 g	a	b	0.5t
19	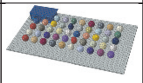	50, 1 layer 5x10	25 mm	0.5 g/cm^3	5,000 N/mm^2	184.1 g	a	b	0.5t
Sect. 2.3.5									
20	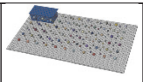	166, 3 layers (5x10, 6x11, 5x10)	6/10/6 mm	0.5 g/cm^3	5,000 N/mm^2	20.6 g	a	b	0.25t
21	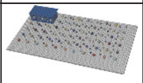	166, 3 layers (5x10, 6x11, 5x10)	6/10/6 mm	5.0/0.5/5.0 g/cm^3	5,000 N/mm^2	71.5 g	a	b	0.25t
22	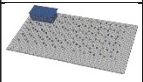	166, 3 layers (5x10, 6x11, 5x10)	6 mm	0.5 g/cm^3	5,000 N/mm^2	8.4 g	a	b	0.25t
23	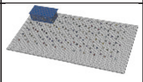	166, 3 layers (5x10, 6x11, 5x10)	6 mm	0.5/5.0/0.5 g/cm^3	5,000 N/mm^2	42.0 g	a	b	0.25t

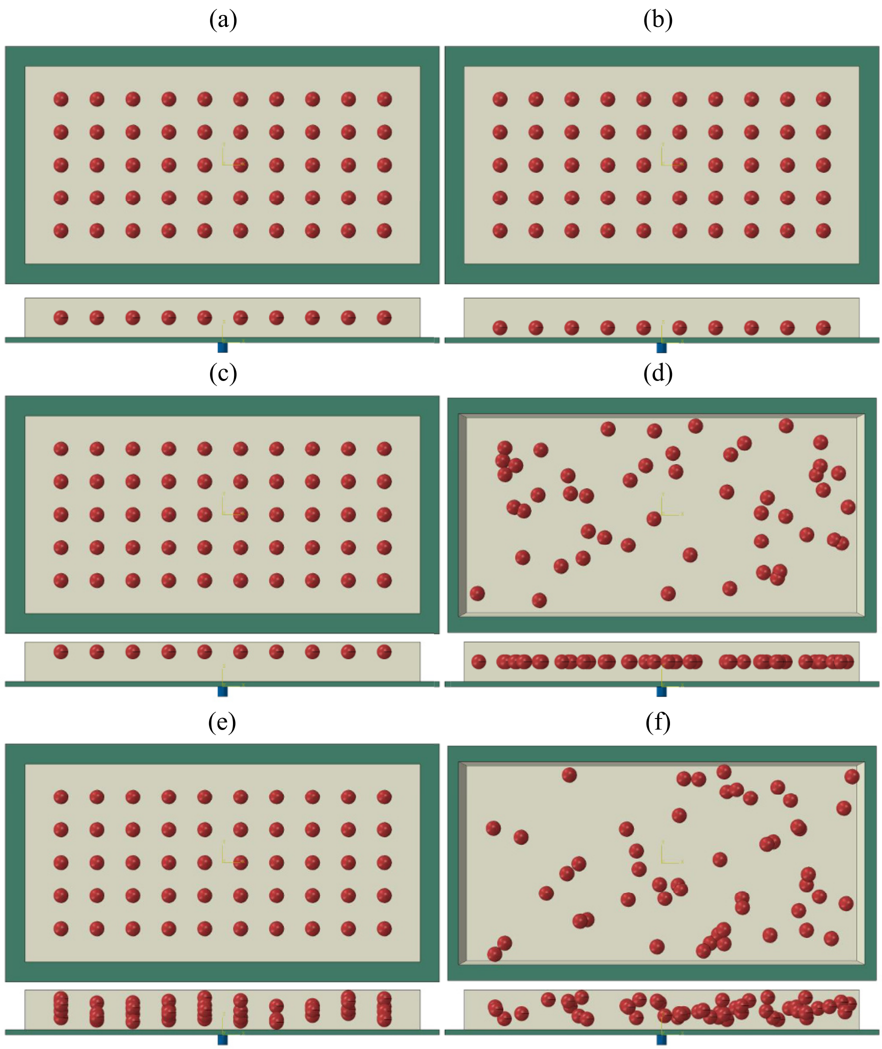

Fig. 2.4: Investigated configurations (top and side view of the sphere position in the foam). The models from Table 2.3 which are used for the analyses are: configuration 1 (a), configuration 2 (b), configuration 3 (c), configuration 4 (d), configuration 5 (e), configuration 6 (f)

Configuration 1 (see Fig. 2.4) is used to generate a reference solution against which all other numerical results are compared in the remainder of the chapter. The results for the sound power level, computed using configuration 1 and a pure PUR foam, are summarized in Fig. 2.5. We observe that the resulting sum level of the A-weighted sound power is decreased by 5 dB(A) when using this simple metamaterial.

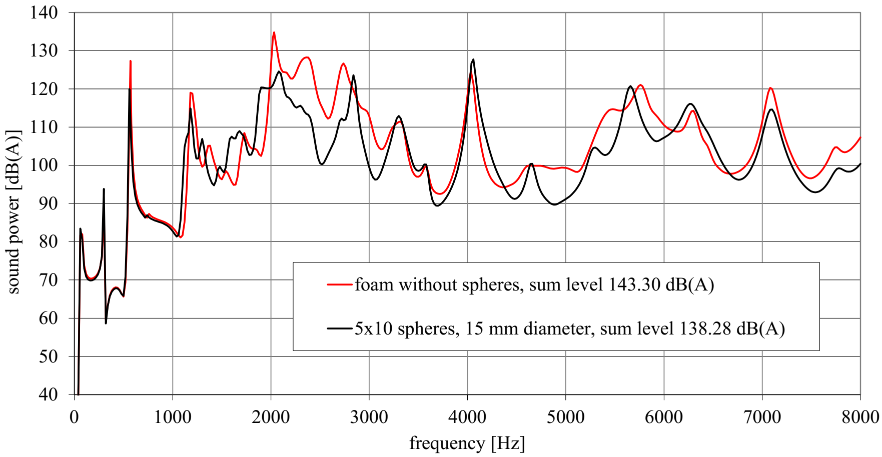

Fig. 2.5: Sound power levels of configuration 1 in comparison to a foam without mass inclusions

The value of the sound power level is calculated on the surface of the hemispherical air volume. Although, a significant overall reduction is generally observed, but there are also small frequency bands where the amplitudes of the sound power level are actually increased by introducing spherical inclusions.

Still the overall results are quite satisfactory with a large amplitude reduction of more than 10 dB(A) between 2 and 3 kHz. If we look at the results of the aluminum plate that is covered with PUR foam only we observe that this frequency band is actually the most critical due to the high amplitudes that are exhibited. Consequently, we were able to achieve the best reduction in amplitudes in a range where it is of special significance for the chosen structure. These remarkable results have been obtained by simply adding inclusions in a structured fashion to an existing damping material.

In the following paragraphs we will settle what advantages can be gained by introducing more advanced arrangements of the spherical inclusions. To this end, the distribution of the 50 spheres is now varied in different steps.

In Fig. 2.6 the computed sound power levels for all six different configurations (see Fig. 2.4) within the frequency interval from 0 to 8 kHz are depicted. In the legend important information such as the distribution of the inclusions and the sum level of the A-weighted sound power are listed. First, we compare the three regular arrangements of the inclusions (see Fig. 2.4 (a) to (c) – configuration 1, 2, 3). In this case, we observe that the best results over the investigated frequency range are obtained, if the spheres are located in the midplane of the plate. Furthermore, we note that a larger distance to the aluminum plate for configuration 3 is advantageous compared to configuration 2 where the spheres are located almost directly above the base plate. However, if we merely consider the sum levels the random distribution in configurations 4 to 6 lead to an improved noise radiation behavior. In our example

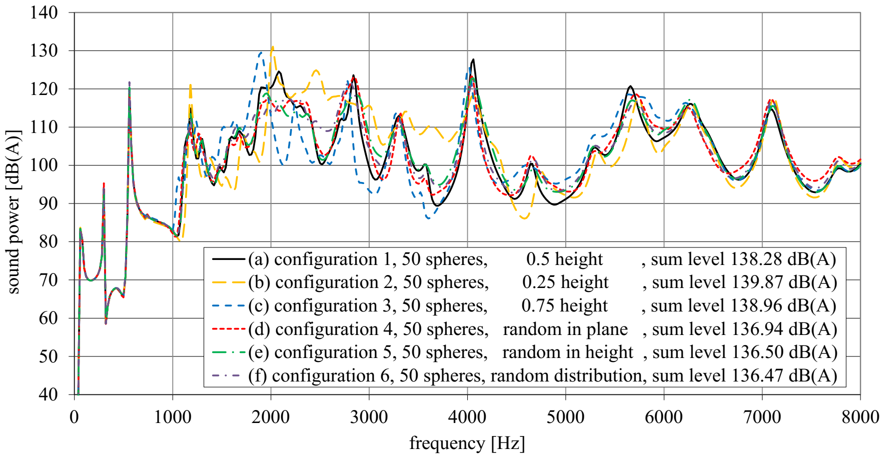

Fig. 2.6: Sound power levels of the configurations 1, 2, 3, 4, 5 and 6

a random distribution over the height while a regular one within the plane is used seems to be a viable choice, as the sum level of configuration 5 is actually almost the same as that of configuration 6. This highlights the fact that the distribution over the height of the damping material is more important than the in-plane one. These findings are also supported by the experimentally drawn conclusions (Schrader et al, 2017b). From a manufacturing point of view (automation of the process) it is also advantageous if a random distribution only needs to be achieved over the height while the in-plane one is structured. Therefore, from our point of view this arrangement constitutes the best choice. In addition, it is remarkable that the behavior in the low frequency range, below 1 kHz, is hardly influenced by the inclusions at all. In the frequency range from 1 kHz to 5 kHz a significant variation in the results can be seen. This is the frequency range where an optimized design can lead to a notable reduction in noise radiation. Above 6 kHz there is again no significant difference between the individual configurations in Fig. 2.6.

2.3.2 Influence of the Material Properties of the Spherical Inclusions

In the current subsection we are going to investigate the influence of the material properties on the noise radiation behavior of the acoustic metamaterial. To this end, the Young's modulus and the mass density of the spherical inclusions are varied for configuration 1 (see Table 2.3). Consequently, configurations 1, 7, 8 ,9 ,10 and 11 are in the focus of this section.

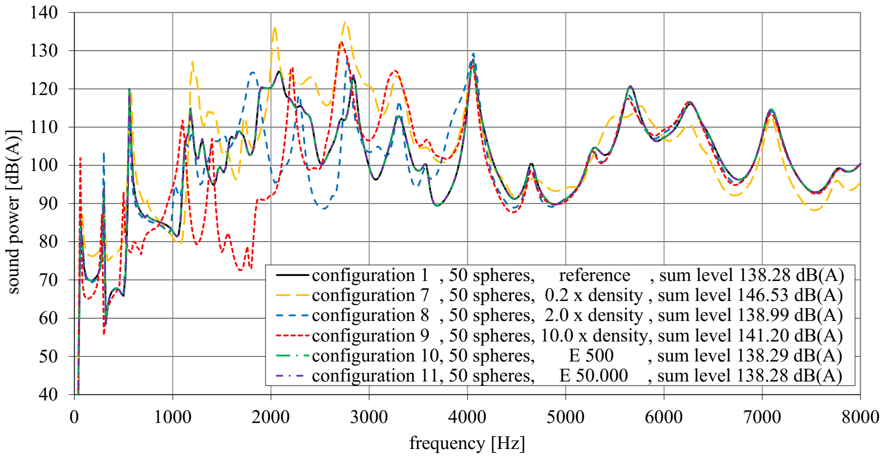

Fig. 2.7: Sound power levels of the configurations 1, 7, 8, 9, 10 and 11 (density and Young's modulus variations based on configuration 1)

In Fig. 2.7 the numerical results for the variation of the material properties are shown. The first conclusion that can be drawn is that the variation of the Young's modulus does not seem to have any notable influence on the results. This behavior can be attributed to the fact that the difference in stiffness between the foam and the inclusions is too large such that the inclusions act as rigid bodies even if the Young's modulus is decreased to only 500 N/mm^2. A second conclusion is that higher density values show an influence on the radiated sound power for frequencies below 4.5 kHz. Only if the density is drastically decreased an effect over the whole investigated frequency range is visible. For our example the lowest chosen density leads to the worst results but also an increased density compared to the initial configuration leads to deteriorated results. This is caused by the fact that these inclusions (with higher density) elevate some resonance peaks in the critical frequency range. This, of course, results in a higher sum level, even if the amplitudes in other frequency ranges are significantly reduced. This behavior is nicely observed in the frequency range from 1.2 to 2.2 kHz where the sound power level is reduced up to 35 dB(A) for the configuration with 10-times the density (dashed red line) and still the computed sum level is rather unsatisfactorily high, as the sum level is dominated almost only by the most important peaks.

2.3.3 Influence of a Fixed Density-Volume-Product

In the next step, the product of density times volume is kept constant, i.e. the added mass is identical for all five different configurations depicted in Fig. 2.8. In our example the additional mass amounts to 39.8 g. The aim of the current investigations

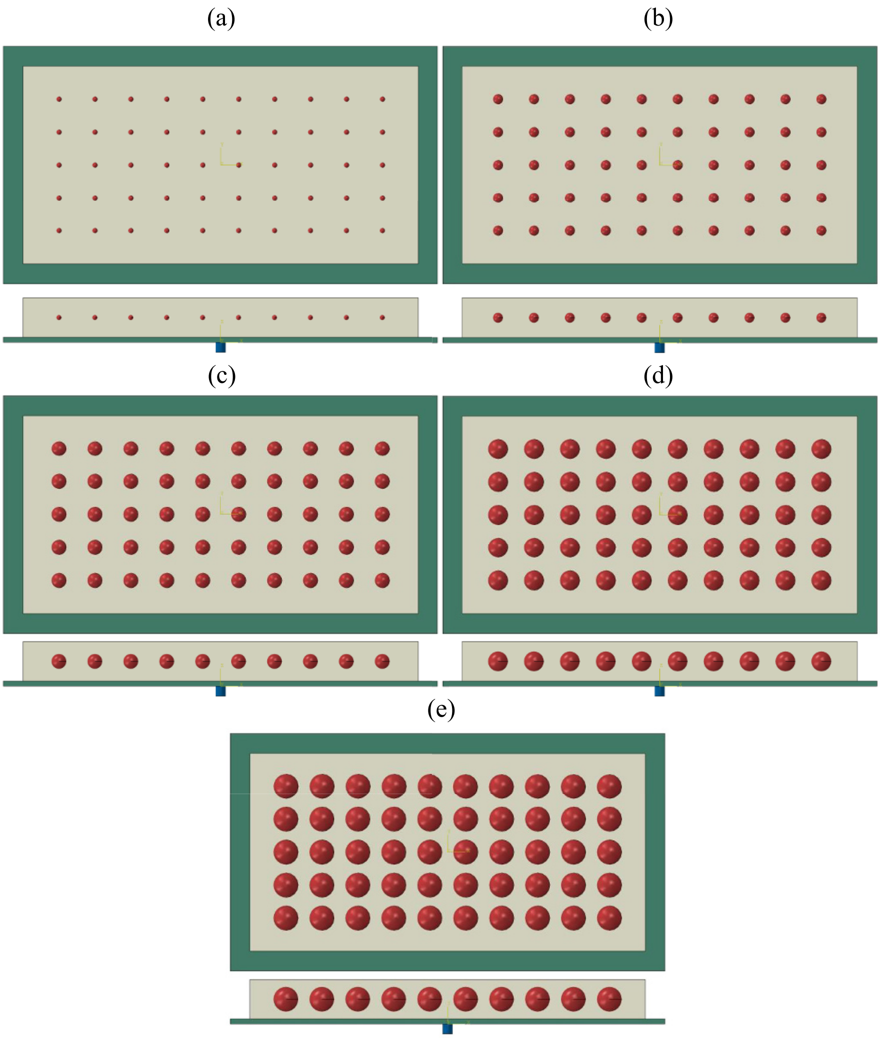

Fig. 2.8: Five different configurations with a fixed density-volume-ratio (top and side view of the sphere position in the foam). The models which are used for the analyses are: configuration 12 (a), configuration 13 (b), configuration 1 (c), configuration 14 (d), configuration 15 (e)

is to answer the question, whether the added mass or the geometrical dimension of the spherical inclusions exerts the dominant influence on the vibration behavior of the structure. If the volume of the sphere is changed, so is the spring constant, assuming that we interpret the inclusion and the foam as a spring-mass-system.

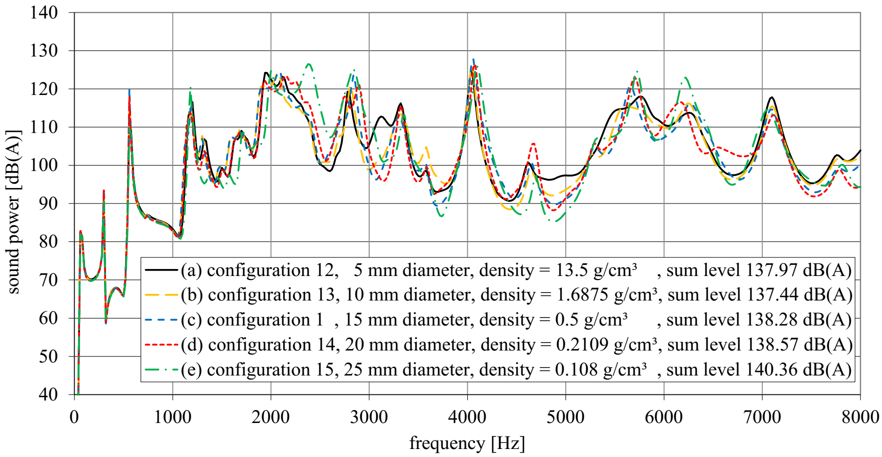

Fig. 2.9: Sound power levels of the configurations 12, 13, 1, 14 and 15 (constant density-volume-product based on configuration 1)

In Fig. 2.9 the computed A-weighted sound power levels for the five configurations depicted in Fig. 2.8 are plotted. It can easily be seen that the qualitative behavior is rather similar, but in some frequency ranges there are significant differences. It can be inferred that larger spheres (with a lower density) seem to be disadvantageous as they considerably reduce the volume of the absorbing foam layer. This in turn also leads to a stiffer spring which increases the eigenfrequency of the single spring-mass system. In the current investigation the spheres with a diameter of 10 mm deliver the best results.

2.3.4 Influence of the Volume of the Inclusions

In the current subsection the five different configurations that have been introduced in Sect. 2.3.3 are studied again, but this time the mass density is fixed to 0.5 g/cm^3 which corresponds to the value of configuration 1 (see Fig. 2.8 (c)). Since now the mass density is constant and volume is different for each example, so are the additional masses. Therefore, the values of the added masses are also given in the legend of Fig. 2.10.

When evaluating the results that are plotted in Fig. 2.10 we note that the configurations 16 and 17 are almost without effect which can be attributed to the negligible additional mass in comparison to the pure foam. Especially in the critical frequency range between 2.0 and 2.8 kHz the vibration behavior is quite poor. However, the two configurations 18 and 19 exhibit large amplitude reductions of up to 20 dB(A) compared to the reference configuration 1. For all that the higher additional masses still cause elevated amplitudes at some other frequencies (e.g. at 2.9, 3.3 or 4.1 kHz).

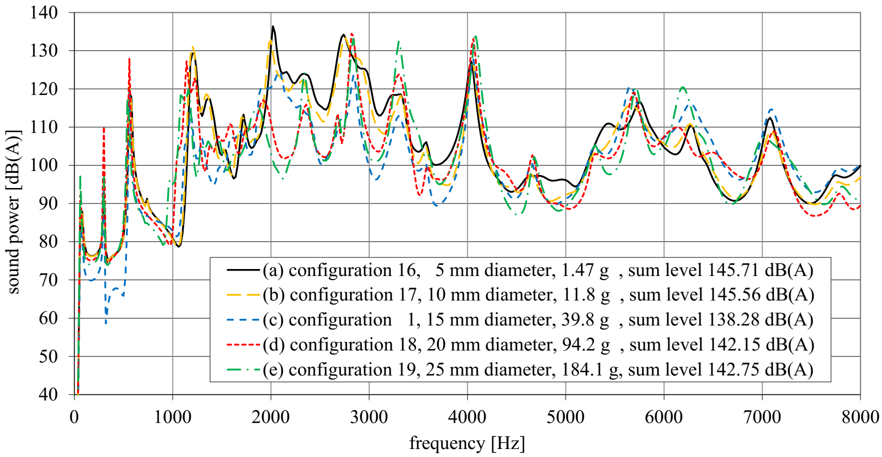

Fig. 2.10: Sound power levels of the configurations 16, 17, 1, 18 and 19 (constant density with different volumes of the spherical inclusions)

This effect can be explained by the fact that large inclusions significantly reduce the volume of the absorbing foam. Thus, the energy dissipation caused by the foam is also decreased. For this reason, we conclude that the spherical inclusions with a diameter of 15 mm are an acceptable compromise for our example.

2.3.5 Influence of the Number of Layers with Different Material Properties

In the current section we investigate the effect of three layers of inclusions where in each layer the spheres are made of a different material. The models are illustrated in Fig. 2.11. In the top and bottom layers again 5x10 spherical inclusions are added to the foam, while in the middle layer 6x11 spheres are used. Consequently, the inclusions in adjacent layers are shifted. The diameter of the inclusions is set to 6 mm for configuration 20 and 21, whereas the two arrangements only differ in the densities of the spheres. Considering the second model, configuration 22 and 23 (different densities of the inclusions), the diameter of all spheres that are in the middle layer is increased to 10 mm. The material properties of the added masses can be taken from Table 2.2. However, note that the density is varied between 0.5 and 5.0 g/cm^3. The actual parameters for each simulation are listed in Table 2.3. In Fig. 2.12 the results for the sound power are depicted. Since the additional mass is an important aspect for such materials, as mentioned in the introduction, it is also given in the legend of that figure.

Surprisingly the results depicted in Fig. 2.12 convey that there is no increased attenuation of the resulting sound radiation due to the number of additional layers and consequently a much higher number of spherical inclusions. Compared to the reference configuration the sound power level is not even slightly reduced but in contrast always elevated for the tested setups. It might be concluded that inclusions with a diameter of only 6 or 10 mm are too small and light (the mass density is 0.5 g/cm^3) to have a significant effect. In the reference configuration spheres with a diameter of 15 mm have been utilized. When the density of the spherical inclusions is increased from 0.5 to 5.0 g/cm^3 they are actually heavier than the inclusions in the reference model and therefore, one might conclude that this distribution of the spheres is detrimental. However, to verify this assumption additional parametric studies need to be conducted. In case the mass density is increased for the outer or the middle layer the damping results are improved but they are still worse than the reference configuration and hold another disadvantage as more mass is added to the system.

2.3.6 Discussion

The conducted parametric studies show that each parameter such as the position, the mass density, the volume and the number of inclusions can have a significant effect on the resulting sound power level. Moreover, we observed that too many or too large inclusions have a negative influence on the radiated sound power. As the overall mass of a passive damping approach is naturally limited, the added mass is also restricted. To find an optimal solution for the presented problem we are

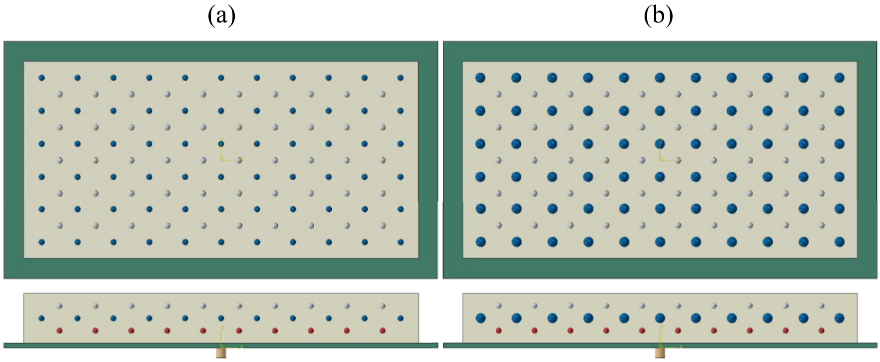

Fig. 2.11: Configurations with three layers of regular positioned mass inclusions, which differ in the material properties and the size of the middle layer. The models which are used for the analyses are: configurations 20, 21 (a) and configurations 22, 23 (b)

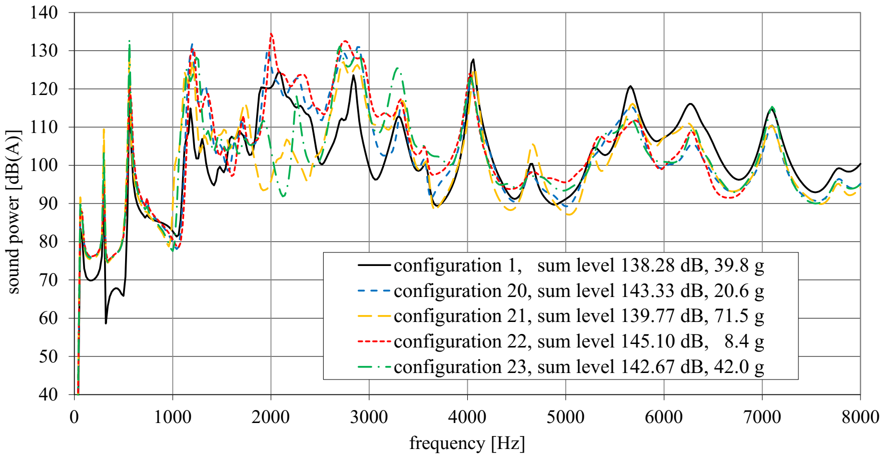

Fig. 2.12: Sound power levels of the configurations 1, 20, 21, 22 and 23

going to deploy computational optimization techniques for future studies. Here, the distribution, the material properties and the geometry of the inclusions will be varied under the constraint of a restricted additional mass and volume. Thus, the potentials and limits of this type of metamaterials can be assessed with respect to its lightweight potential and achievable sound reduction.

The observations reported in the contribution at hand are supported by experimental findings that have been published in Schrader et al (2017a). In comparable experimental measurements it was shown that an arrangement of inclusions far from the damped surface leads to an increased damping effect in a higher frequency range (Schrader et al, 2017a). Furthermore, a concept with a large number of added masses was rejected as being inefficient (Schrader et al, 2017a) similar to the results presented in Sect. 2.3.5.

2.4 Conclusions

In this contribution we investigated the potential of a special class of acoustic metamaterials by means of numerical simulations (FEM). Our focus lay on locally resonant structures consisting of an elastic matrix material in combination with spherical inclusions (added masses). Our exemplary application case is a soft synthetic foam made of polyurethane with much stiffer inclusions within. These inclusions have been varied in size, material properties, number and position. Here, it was shown that this type of acoustic metamaterials is well suited to increase the damping effect compared to that of the base material. Depending on the tuned arrangement of inclusions it is both possible to influence the damping properties only in certain frequency bands or over the whole frequency range of interest. A strong correlation between the influence parameters of the spherical mass inclusions (size, material properties, number and position) and the resulting sound power level was observed. That is to say, we have to be careful when designing such an acoustic metamaterial as an arbitrary distribution of inclusions with arbitrary parameters could result in a worse performance compared to the base material. Consequently, it is of utmost importance to design efficient and robust numerical tools for the dimensioning of these materials. A first step in this direction was made in this contribution.

In the parametric studies we observed that the stiffness of the inclusions has a negligible effect on the achieved sound absorption. Due to the vastly different mechanical impedances of both materials all investigated inclusions acted as rigid bodies within the soft elastic foam. On the other hand, a variation of the mass density of the spherical inclusions or their location cause a significant difference in the radiated sound power in a frequency range between 1 and 5 kHz. Both below 1 kHz and above 6 kHz the different tested configurations displayed hardly any changes in the resulting sound power levels. For our example problem the sound radiation is deteriorated if the mass density is chosen too high or too low. Consequently, this parameter should be optimized for future applications. Moreover, it was verified that the product of mass density and volume has an influence on the sound absorption. In this context, it has been found that the spherical inclusions should be neither to small nor to big as the obtained results have been much worse compared to our reference configuration. For this reason, the size of the inclusions is a second parameter that calls for an optimization. In regard to the positioning of the inclusions we can state that the out-of-plane direction is seemingly more important than the in-plane directions. Therefore, the position might be a third parameter that should be investigated by means of a numerical optimization technique, although random distributions have in general attained favorable results in our parametric studies.

Finally, the presented results have been validated with experimental measurements that have been published previously. The most important conclusions that we have drawn from the parametric studies are supported by the experimental evidence. With the help of the knowledge derived from the observations of this contribution initial design proposals for this class of acoustic metamaterials can be given. Therewith, we are able to achieve an improved damping behavior with a minimum gain in mass.

Future research activities in the direction of acoustic metamaterials will include a fully automated numerical optimization to determine the optimal configuration. To this end, a sophisticated python script has been developed to automatically generate the finite element model for arbitrary arrangements. The parameters that should be included in the optimization process are the number of inclusions, the number of layers, the size, the position and the material properties of the inclusions. The objective function will be the resulting sound power level of the overall system. We hope that the results of the optimization process will help us to answer the following questions:

1. How many inclusions should be added to the base material?
2. How many layers of inclusions should be added?
3. Which distribution of inclusions should be deployed to obtain the best possible results?

4. Which material should be chosen for the inclusions?

In the current study it was demonstrated that one layer featuring 50 spherical inclusions performs better than several layers with a much greater number of added masses. In general, this might not be true considering that the randomly distributed configurations lead to the best overall results.

After the numerical optimization has been executed a prototype of the optimal configuration will be produced and compared to both the best configurations determined in the current contribution and to the foam material without any modifications. The experimental measurements will be conducted in an acoustic far field room which is equipped with a microphone array and far field microphones. The aim is to validate that the computed optimal solution exhibits a significantly improved damping behavior compared to all other previous configurations.

Another interesting point for future studies is naturally the investigation of the influence of the inclusion shape on the damping behavior. Therefore, different simple shapes such as arbitrary ellipsoids could be studied in contrast to arbitrarily shaped (convex) inclusions generated by means of Voronoi diagrams.

Acknowledgements The presented work is part of the joint project COMO "Competence in Mobility", which is financially supported by the European Funds for Regional Development (EFRE) as well as the German State of Saxony-Anhalt. This support is gratefully acknowledged.

We would also like to thank our colleague Peter Schrader from the Institute of Mobile Systems (Otto-von-Guericke-Universität Magdeburg) for numerous fruitful discussions, the successful cooperation during the last years and the execution of the experiments, which supported our efforts to gain a deeper insight into the acoustical behavior of metamaterials and their most important influence parameters.

References

Deymier PA (2013) Acoustic Metamaterials and Phononic Crystals. Springer-Verlag Berlin Heidelberg

Duvigneau F (2017) Ganzheitliche simulationsbasierte Bewertung der Akustik von automobilen Antrieben. No. 467 in Fortschritt-Berichte VDI, Reihe 20, VDI-Verlag GmbH, Düsseldorf

Duvigneau F, Koch S, Woschke E, Gabbert U (2016a) An effective vibration reduction concept for automotive applications based on granular-filled cavities. Journal of Vibration and Control

Duvigneau F, Liefold S, Höchstetter M, Verhey JL, Gabbert U (2016b) Analysis of simulated engine sounds using a psychoacoustic model. Journal of Sound and Vibration 366:544–555

Duvigneau F, Luft T, Hots J, Verhey JL, Rottengruber H, Gabbert U (2016c) Thermo-acoustic performance of full engine encapsulations - a numerical, experimental and psychoacoustic study. Journal of Applied Acoustics 102:79–87

Duvigneau F, Nitzschke S, Woschke E, Gabbert U (2016d) A holistic approach for the vibration and acoustic analysis of combustion engines including hydrodynamic interactions. Archive of Applied Mechanics 86(11):1887–1900

Fuchs HV (2007) Schallabsorber und Schalldämpfer. Springer-Verlag Berlin Heidelberg New York

Fuller C, Saux TD (2012) Sound absorption using poro-elastic acoustic metamaterials. In: Internoise 2012 conference proceedings

Gabbert U, Duvigneau F, Ringwelski S (2017) Noise control of vehicle drive systems. FACTA UNIVERSITATIS, Series: Mechanical Engineering 15(2):183–200

Givoli D (2008) Computational absorbing boundaries. In: Marburg S, Nolte B (eds) Computational Acoustics of Noise Propagation in Fluids, Springer-Verlag, Berlin, pp 145–166

Hughes TJR (1987) The Finite Element Method: Linear Static and Dynamic Finite Element Analysis. Prentice-Hall, New Jersey

Idrisi K, Johnson ME, Theurich D, Carneal JP (2010) A study on the characteristic behavior of mass inclusions added to a poro-elastic layers. Journal of Sound and Vibration 329:4136–4148

Jensen JS (2011) Waves and vibrations in inhomogeneous structures: Bandgaps and optimal designs. PhD thesis, Technical University of Denmark

Koch S, Duvigneau F, Duczek S, Woschke E (2017a) Vibration reduction in automotive applications based on the damping effect of granular material. In: Automotive Acoustics Conference 2017, 4. Internationale ATZ-Fachtagung Fahrzeugakustik

Koch S, Duvigneau F, Orszulik R, Gabbert U, Woschke E (2017b) Partial filling of a honeycomb structure by granular materials for vibration and noise reduction. Journal of Sound and Vibration 393:30–40, DOI http://dx.doi.org/10.1016/j.jsv.2016.11.024

Liu Z, Zhang X, Mao Y, Zhu YY, Yang Z, Chan CT, Sheng P (2000) Locally resonant sonic materials. Science 289:1734–1736

Liu Z, Chan CT, Sheng P (2005) Analytic model of phononic crystals with local resonances. Physical Review B 71:1–8

Lu MH, Feng L, Chen YF (2009) Phononic crystals and acoustic metamaterials. Materials today 12:34–42

Maa DY (1998) Potential of microperforated panel absorber. Journal of the Acoustical Society of America 104:2861–2866

Ringwelski S, Luft T, Gabbert U (2011) Piezoelectric controlled noise attenuation of engineering systems. Journal of Theoretical and applied mechanics 49(3):859–878

Schirmacher R, Lippold R, Steinbach F, Walter F (2007) Praktische Aspekte beim Einsatz von ANC-Systemen in PKW. In: Fortschritte der Akustik, DAGA

Schrader P, Duvigneau F, Luft T, Gabbert U, Rottengruber H (2015) Development, Simulation and Experimental Investigation of a Function-Integrated and Foam Damped Oil Pan for a Two Cylinder Diesel Engine. In: 44th International Congress and Exposition on Noise Control Engineering - InterNoise 2015, San Francisco

Schrader P, Duvigneau F, Orszulik R, Rottengruber H, Gabbert U (2016) A numerical and experimental study on the noise absorption behavior of functionally graded materials considering geometrical and material influences. In: 45th International Congress and Exposition on Noise Control Engineering - InterNoise

Schrader P, Duvigneau F, Rottengruber H, Gabbert U (2017a) The noise reduction potential of lightweight acoustic metamaterials Ű a numerical and experimental study. In: Automotive Acoustics Conference 2017, 4. Internationale ATZ-Fachtagung Fahrzeugakustik

Schrader P, Duvigneau F, Rottengruber H, Gabbert U (2017b) Passive Reduktion der Schallabstrahlung von Oberflächen durch Anwendung von Metamaterialstrukturen. In: 43. Jahrestagung für Akustik - DAGA

Sheng P, Mei J, Liu Z, Wen W (2017) Dynamic mass density and acoustic metamaterials. Physica B 394:256–261

Sui N, Yan X, Huang TY, Xu J, Yuan FG, Jing Y (2015) A lightweight yet sound-proof honeycomb acoustic metamaterial. Applied Physics Letters 106:1–4

Troge J, Drossel WG, Lochmahr M, Zumach S (2016) Reducing rear axle gear whine noise inside a car by influencing the structure-borne sound transfer path using structurally integrated piezo-actuators. In: Proceedings of the 22nd International Congress on Acoustics - ICA

Zhang G, Jackson T, Lafond E, Deymier P, Vasseur J (2006) Evidence of surface acoustic wave band gaps in the phononic crystals created on thin plates. Applied Physics Letters 88:3pp.

Zhang ZM, Gu XT (1997) The theoretical and application study on a double layer microperforated sound absorption structure. Journal of Sound and Vibration 215:399–405

Zhao M, Xie YZ, Zhang XG, Gao J (2013) Band gaps of Lamb waves propagating in one-dimensional periodic and nesting Fibonacci superlattices thin plates. Thin Solid Films 546:439–442

Zienkiewicz OC, Taylor RL (2000) The Finite Element Method: Volume 1 The Basis. Butterworth Heinemann, London

http://www.springer.com/978-981-10-6764-8

Analysis and Modelling of Advanced Structures and Smart Systems
Altenbach, H.; Carrera, E.; Kulikov, G. (Eds.)
2018, XVIII, 366 p. 192 illus., 72 illus. in color., Hardcover
ISBN: 978-981-10-6764-8